Chapter 1

Soft Wearable Assistive Robotics: Exosuits and Supernumerary Limbs

Lorenzo Masia [1], Irfan Hussain[2 3], Michele Xiloyannis[1], Claudio Pacchierotti[4], Leonardo Cappello [5] , Monica Malvezzi [2], Giovanni Spagnoletti[2], Chris Wilson Antuvan[1], Dinh Binh Khanh[1], Maria Pozzi[2] and Domenico Prattichizzo[2 6]

Abstract

The intrinsic soft nature of compliant supernumerary limbs and exosuits makes them appealing candidates for assisting human movements, with potential applications in healthcare, human augmentation and logistics. In the following chapter, we describe the technology used in exosuits and supernumerary limbs for assistance of activities of daily living, with emphasis on aiding grasping and flexion/extension of the elbow joint. We discuss the mechanical design principles of such devices, detail the control paradigms that can be used for intention-detection and present the design and evaluation of cutaneous interfaces used for force feedback rendering. Tests on healthy and impaired subjects highlight that exosuits and supernumerary limbs are potential cost-effective and intrinsically safe solutions for increasing the capabilities of healthy subjects and improving the quality of life of subjects suffering from motor disorders.

Keywords:Assistive Devices, Wearable Robots, Rehabilitation Robotics, Medical Robots, Soft Material Robotics

[1]Robotics Research Center, Nanyang Technological University, Singapore
[2]Dept.Information Eng.and Mathematics,University of Siena,Siena,Italy
[3]Khalifa University Robotics Institute, Khalifa University of Science Technology and Research, Abu Dhabi, United Arab Emirates
[4]CNRS, Univ Rennes, Inria, IRISA, France
[5]The Biorobotics Institute, Scuola Superiore SantAnna, Pisa, Italy
[6]Dept. Advanced Robotics,Istituto Italiano di Tecnologia,Genoa,Italy

1.1 Introduction

The introduction of compliant elements in robotics revolutionized the path to the design of applications with human in the loop; series elastic actuation [1] was the ignition to this new approach which has been widely accepted by a large part of the robotic community that considered the use of compliant elements as the natural solution to solve the problem of human robot-interaction.

Haptics, robot-aided rehabilitation and assistive technology embraced the new idea of designing devices which included compliance among the joints and at the end effector, with the final purpose to optimize the human interaction by reducing the contact force and filtering fast and abrupt dynamics. Literature reports a multitude of devices employing series elastic [2], pneumatic [3] and variable impedance actuators [4] which found their natural application in rehabilitation [5], telemanipulation [6] and in general for all those tasks which can benefit from force limitation and fine regulation of the interaction at the end effector.

Compliant actuation opened a new scenario, alternative to the classic robotics precept "stiffer is better"; a new control approach was adopted with the purpose of transforming the force problem into a position problem where the deformation of the compliant element was the main indicator of the interaction forces between the human and robotic device. Rehabilitation robotics and assistive technology were the applications which benefited most from the new gentle approach. Worldwide scenario comprises two different approaches which are mainly driven by the residual capacity of motion from the final users.

Technology for rehabilitation and assistance has principally targeted Stroke as the leading cause of permanent disability worldwide and its efficacy is strictly linked to the mutual interaction between the patient and the devices.

Despite the large diffusion there are still several drawbacks which are far from solved, especially in assistive technology. The aforementioned improvements in actuation and control solutions did not prevent the majority of devices from employing rigid components in parallel with the human biomechanics, with a resulting ergonomics and usability which are still far from nearly optimal. Furthermore, the weight of the current devices requires unacceptable metabolic costs from the wearer, with a consequence movement restriction imposed on the user's joints which may result in misalignment and parasitic torques on the articulations.

Soft wearable exoskeletons (or exosuit) and Supernumerary Robotics are the successive step to the introduction of compliant actuation, where not only the actuators but also the structure of the device itself is designed to be compliant. This new vision has been gradually arousing the interest of the robotic community, proving to be a viable complementary solution to rigid robotics. Whilst not being suitable for the applications requiring large forces and torques where rigid devices still show higher performance, exosuits' and supernumerary limbs' intrinsic compliance, portability and low-power consumption make them ideal for partly augmenting the muscular strength or providing additional support in activities of daily living such as walking [7, 8, 9], hand grasping [10] and stabilization tasks [11].

Exosuits overcome the limitations introduced by the conventional exoskeletons, where the lack of mechanical compliance in their kinematic structure represents the main factor limiting a wider diffusion of such technology.

As an alternative to the stiff links of conventional exoskeletons, the exosuit design comprises fabrics and meta-materials to connect the human limb to the actuation stage, while the support is demanded to the human musculoskeletal system: this solution results particularly suitable in those applications where the human biomechanics is able to provide a supporting structure while actuation and transmission can deliver torque and force across the human articulations [12].

There are not many examples of exosuits in the literature and the majority are focused on lower limb. Due to the cyclic nature of walking, the great control challenge is triggering the assistance at the right phase of walking, and delivering it to the correct anatomical joints which are usually restricted in the sagittal plane of motion: examples of exosuit used in delivering assistance to both healthy and impaired subjects are from Panizzolo and Rossi *et al.* [8, 13] where a bowden cable-driven exosuit for ankle and hip assistance has been used on stroke subjects showing tangible benefits in improvement of metabolic costs and walking efficiency.

One of the most significant examples of an upper limb exosuit, which employed a fine model-based controller implementation, was from Ueda *et al.* and Ding *et al.* [14, 15]; consisting in a wearable fully compliant exosuit at the shoulder/elbow joints. The device was driven by flexible pneumatic actuators with ends anchored to rigid plastic frames, and equipped with force and EMG transducers to apply force feedback control. The novelty of the design was in the integrated human-exoskeleton model used to compute the interaction between the human muscle forces and torques generated by the exosuit.

Other examples of wearable textile-garment based exosuits for hand rehabilitation come from Lee *et al.* [16] and In *et al.* [17], where and exotendon device and exo-glove respectively, used cable actuation to promote the recovery of fingers coordination and restoring functional hand movement after stroke or spinal cord injury. The two devices used different approaches: the exotendon has been designed to be a rehabilitation device for clinical therapy, where the geometry and the disposition of the tendons, driven by seven motors, aimed at finely replicating different hand gestures (i.e. grasping, lateral grip, pinching etc.) with a passive motion paradigm; the exo-glove relied on a more compact design, employing an underactuated mechanism by Jeong *et al.* and focusing its strength on the portability and versatility, where assistance was triggered by wrist motion detection.

Supernumerary Limbs contrarily to the exosuits are not mounted in parallel respect to the human articulations but they are additional limbs. The main function of such architectures is not intended to provide additional torque at the level of human joints but mostly to replace the lost functionality, improving the dexterity of the users.

Supernumerary Robotic Limbs (SRLs) were initially conceived for industrial applications; attached to the human waist to support the body, powered joints were attached to the human joints and are constrained to move together with the human limb. The SRLs are designed to take a set of postures to maximize the load bear-

ing efficiency. The SRLs can bear a large load with small power consumption and provide the users with additional dexterity which can facilitate a specific set of tasks.

Supernumerary Limbs have been also been recently employed on impaired subjects: more specifically when the level of neurological impairment is severe and the patient's residual capacity of motion is too low, supernumerary robotics represents a complementary option to regular exoskeletons and exosuits. For example, patients affected by hypertonia or muscular atrophy due to a prolonged limb immobilization, will be unable to use an exoskeletal structure, because of the lack of biosignals useful to drive/trigger the exosuits, and their compromised biomechanics which avoid the exoskeleton to properly works (i.e. joint misalignment and residual muscular cocontraction).

For the above mentioned reasons supernumerary limbs represents a viable option to provide severely affected patients with an additional dexterity, which is able to partly restore the functionality of a limb and allow them to perform basic activities of daily living which before would have been almost impossible.

The following sections will describe the technology used in exosuits and supernumerary limb applications. Examples and previous work from the authors will provide an overview of the potentials and limitations of such technology, highlighting their complementarity and possible future trends.

1.2 Exosuits

A wealth of devices has been engineered to assist the upper-limbs in physical therapy [18, 19, 20, 21, 22, 23, 24, 25, 26, 27] mostly consisting of load-bearing exoskeletons made of rigid links that operate in parallel to the human skeleton.

One of the most common limitations of these exoskeletons is given by the kinematic constrains imposed on the wearer's joints by the rigid frame. Misalignment between the robot's joints and the biological ones results in hyperstaticity [28], i.e. the application of uncontrolled interaction forces, which upsets the natural kinematics of human movements. Various methods have been proposed to avoid hyperstaticity, such as adding passive DOFs [29], self-aligning mechanisms [30] or remote centres of rotation [31]. These solutions come at the cost of increasing the size and mass of the device, which makes it intrinsically unsafe and thus unsuitable for unsupervised, at-home use.

A recent and promising paradigm consists of delivering forces to the human skeletal system by means of soft, clothing-like frames powered either by pressurizable elastomeric actuators [32, 33, 3, 34, 35] or by bowden cables moved by proximally-located motors [36, 37, 12, 17].

The use of clothing-like frames, known as *exosuits*, for transmitting forces to the human body represents an appealing solution for human motion assistance. Their intrinsic compliance, low profile and quasi-negligible inertia make them likely candidates for use on a daily-basis. The absence of a rigid structure, moreover, avoids the joint-misalignment problem and makes the device completely transparent to human kinematics.

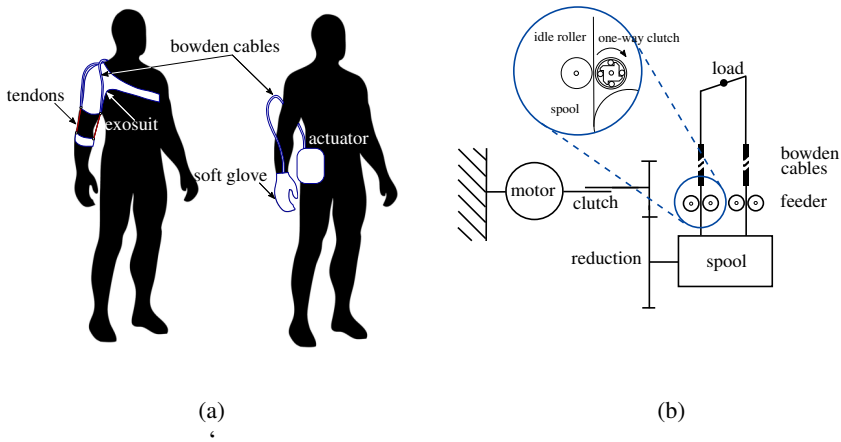

Figure 1.1: Components of the exosuits (a) and schematics of the actuation units (b). (a) Both devices comprise a wearable component (exosuit or glove) and a proximally-located actuation unit that transmits power to the joints via bowden cables. (b) DC brushless motors drive a spool around which the artificial tendons are wrapped; an electromechanical clutch allows to couple and decouple the motor from the transmission, allowing the user to move freely on demand. A feeder mechanism, thoroughly described by In *et al.*[38], keeps the cables in tension around the spool.

The downside of exosuits is their inability to apply high forces: being there no external rigid frame, loads are born by the wearer's joints. Nevertheless Quinlivan *et al.* have demonstrated that applying small forces with the correct timing during the walking cycle can reduce the metabolic cost of walking [9] up to 22.83% with no reported damage on the user's joints and In *et al.*, have experimented with a soft glove with a bio-inspired tendon routing on a tetraplegic patient for restoring up to a 50N hand grasp [17].

1.2.1 Design and Actuation

The elbow and the hand exosuits comprise an actuation stage and a wearable component. The actuation stages are located proximally (e.g. in a belt around the waist) and transmit power to the suits via bowden cables (Figure 1.1a).

Both tendon-driving units follow the same working principle, schematically shown in Figure 1.1b: a brushless DC motor drives a spool around which one or more pairs of artificial tendons are wrapped in an antagonistic fashion so that rotation of the motor in one direction causes retraction of the agonist cable and releases its antagonist. An electromagnetic clutch is placed in between the motor shaft and the spool, coupling and uncoupling the motor and the end-effector when engaged and disengaged respectively. This allows the controller to switch from a driving mode, where the exosuit is assisting its wearer, to a *transparent* mode, where the suit acts as a garment and allows free and unconstrained movements.

It is important to guarantee that the tendons don't slack around the spool. Pretensioning, a strategy commonly used in tendon-driven robots [39], is not a feasible solution due to the stress that a continuous force would introduce on human joints: rather, we adopt a feeder mechanism, thoroughly described in [38], that confines the slack outside of the actuation unit.

The feeder mechanism comprises two idle rollers and two one-way clutches. The tendons pass between the rollers and the clutches. The one-way clutches' shaft is coupled to the spool's shaft with a spur gear. When the cable is released, the one-way clutches are engaged, thus pulling the cables out and keeping the tension around the spool. When the cable is retracted, the one-way clutches are idle and the feeder mechanism does not interfere with the re-wrapping of the cable. In order to increase adhesion, a lining of urethane coating was added on the metallic surface of the one-way clutches.

The elbow actuator (shown in Figure 1.2a) comprises the following components: a brushless motor (Maxon EC-max, ∅ 22mm, 50W) coupled to a gearhead (reduction of 33:1) and whose position is sensed by a quadrature encoder (Maxon Encoder MR, 512 CP), a spool around which two cables are coiled in opposite directions, a feeder mechanism and an electromagnetic clutch (Inertia Dynamics, SO11).

The two tendons, made of superelastic NiTi wire, were routed from the actuator unit on the backpack to the elbow joint through an outer cable housing (Nokon, Sava Industries). The whole mechanism is enclosed in a 3D printed case in ABS plastic. The fundamental components of the actuator driving the cables of the soft glove for grasp assistance are shown in Figure 1.2b. Schematically, this unit is exactly

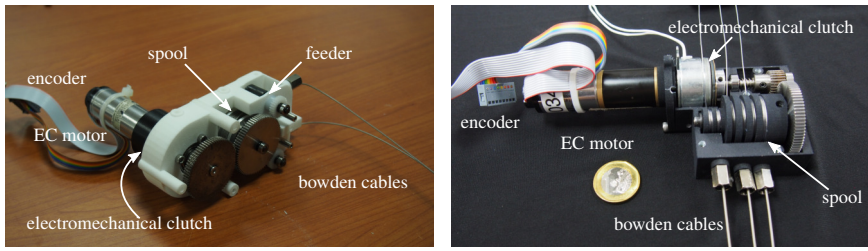

(a) (b)

Figure 1.2: Tendon-driving units for the elbow sleeve (a) and the glove (b). Both actuators follow the design schematized in Figure 1.1b, enclosed in a 3D printed plastic casing. The elbow and hand units weight, respectively, 750g and 420g.

like the one for the elbow, modelled in Figure 1.1b, with the only difference that it drives three pairs of antagonistic tendons instead of one. The device consists of a DC brushless motor (Maxon EC-max, ∅ 22mm, 25Watt) equipped with a rotary encoder (Maxon Encoder MR, 512 CPT) and a planetary gearhead with a reduction of 23:1. A further 3:1 reduction between the motor and the spool shaft ensures that the electromechanical clutch (Inertia Dynamics, SO11, $\tau_{max} = 0.68$Nm) can withstand higher locking torques.

The exosuit for the elbow (shown in Figure 1.3) was designed by modifying a commercially available passive orthosis (MASTER-03, Reh4mat). The substrate of the suit, having the function of adhering to the body of the user and keeping it in place, is made of a 3-layered fabric: an external layer used to attach hard components (buckles and webbing strips), an intermediate Ethylene-vinyl acetate (EVA) foam cushions high loads and avoids high pressures and an internal 3D polyamid structure provides high air permeability and moisture absorption. Additionally the arm bands are lined with a silicone pattern at the interface with the skin to prevent slipping. Load paths, i.e. the directions along which forces are transmitted through the fabric to the body, need to be as stiff as possible to maximize force transmission efficiency. They are thus made of webbing, i.e. nylon fibers woven in a flat strip, which is virtually inextensible and able to support high loads. To route the tendons along the load paths we sewed 3D printed components on the webbing network on both sides of each joint. These serve as artificial ligaments, anchoring the tendons to the body.

Finally, pre-tensioning the suit against the body, fundamental to avoid slipping and increase transmission efficiency, is achieved via buckles and velcro straps around the arm and forearm and along the load-paths (Figure 1.3). In Figure 1.3.b the subject is also wearing a harness designed to carry the actuation unit on his torso. The harness, that can be tightened through a set of buckles, loads the weight of the device (≈2kg including actuation, electronics and power supply) on the wearer's shoulders.

The soft glove for grasping assistance (shown in Figure 1.4) is designed following the same principles. An elastic lycra layer forms the substrate of the glove, ensuring a snug fit and keeping the anchor points in place while a neoprene layer ensures comfort where the major forces are applied by the tendons. The anchor points,

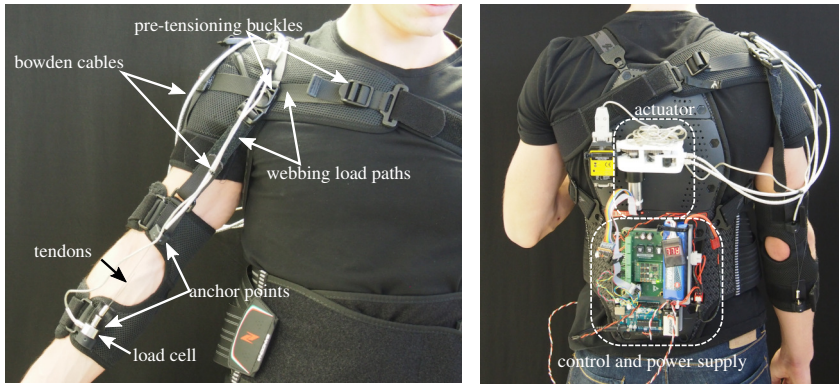

(a) (b)

Figure 1.3: Anterior and posterior views of the exosuit for assisting elbow flexion/extension motions. (a) The artificial tendons are routed in a pair of bowden sheaths from the actuator to the elbow joint; anchor points, on both sides of the joint, attach the tendons to the body, behaving like ligaments, and can be tightened with buckles and a velcro strap. Loads are directed along paths made of unstretchable fabric that can be pre-tensioned around the body of the wearer upon donning. (b) The actuator, the electronics and the power supply are carried in a backpack-fashion and weighs, overall, 2.1 Kg.

driving the tendons along the phalanxes and between the joints, are 3D printed in ABS and sewn on the fabric.

A wrist brace and the fingertip fittings are essential for an effective transmission of forces to the body since they are the only points where forces are applied normally to the skeletal structure. Specifically, the wrist brace loads the protruding trapezium and pisiform bones on the wrist and the fingertip fittings act on the distal phalanx of each finger. A pair of velcro straps facilitate donning and doffing of the glove.
Table 1.1 summarizes the overall weight and materials cost of the exosuit and the glove.

Table 1.1: Weight and cost of the exosuit and the glove

	Elbow[Kg]	**Hand**[Kg]	**Elbow**[US $]	**Hand**[US $]
Actuation	0.750	0.420	970	662
Power Supply	0.695	0.242	44	23
Electronics	0.270	0.270	222	222
Suit	0.397	0.205	123	97
Total	2.112	1.137	1359	1004

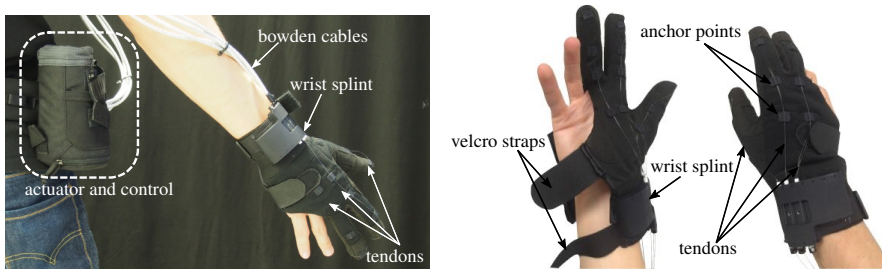

Figure 1.4: Soft glove for grasping assistance; dorsal and palmar view. The glove combines three different fabrics and rigid anchor points to be both comfortable and functional. A substrate in elastic fabric guarantees a snug fit, thus avoiding slipping of the anchor points during usage. A layer of neoprene, under the anchor points, avoids the application of high pressures on the wearer's skin. A pair of velcro straps facilitates donning and doffing.

1.2.2 Control

While the use of flexible materials for transmitting forces to the wearer presents many advantages, it also poses unquestionable control challenges: deformation of stretchable materials, friction in the bowden cables and the viscoelastic properties of human soft tissues make a simple feedback control inadequate for achieving a reasonable tracking accuracy. Moreover, understanding the the intentions of the wearer is a key but challenging task.

We propose to tackle these issues by implementing a layered control paradigm which intuitively operates the exosuit. The proposed controller, shown in Figure **??**, is referred to as *hierarchical* because it consists of three separate layers in cascade. We aim at considering all the aspects ranging from human intention detection for assistance evaluation (high layer), to adaptive compensation of unwanted effects arising from the presence of non linear behaviours in the exosuit (low layer). We test the proposed hierarchical control architecture in a trajectory following task an quantify its level of assistance on healthy subjects by monitoring the Electromyographic (EMG) activity of the muscles involved.

1.2.2.1 High Level Controller

The high level controller deals with the task of understanding the intention of the user, converting it into an estimated torque at the joint and successively into a joint position using a dynamic model of the human arm. To do so we used a mathematical model for bowden-cable transmission that provides an acceptable estimation of the torque from the cable tensions [40] measured by load cells shown in Figure 1.3. Using simple geometrical considerations, we can derive the *extension functions* $h_i(\phi_e)$

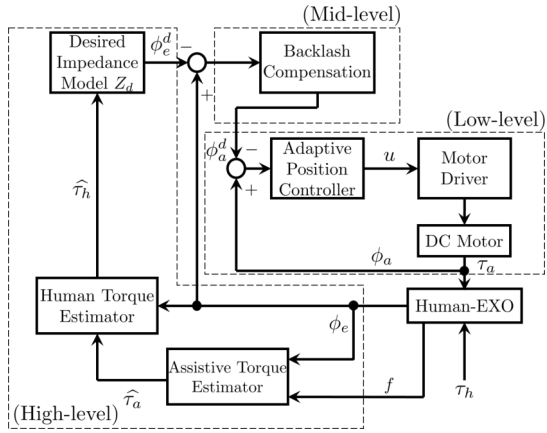

Figure 1.5: Schematics of the controller's architecture. The controller comprises three layers: a high-level one to decode the subject's intention and modulate the level of assistance; a middle-layer to compensate for backlash in the Bowden cable and a low-level controller to compensate for static and dynamic friction in the transmission.

mapping the cables (flexor and extensor) displacement to the joint angle ϕ_e. The flexor cable has an extension function $h_1(\phi_e)$ defined as:

$$h_1(\phi_e) = 2\sqrt{a^2+b^2}\cos\left(\tan^{-1}\left(\frac{a}{b}\right)+\frac{\phi_e}{2}\right)-2b \tag{1.1}$$

while the extensor cable is described by:

$$h_2(\phi_e) = R\phi_e \tag{1.2}$$

where a is half of the width of the arm, b is the distance from the joint centre of rotation to the anchor points (rigid braces), R is the radius of the elbow joint, and ϕ_e is the elbow joint angle. From the two extension functions $h_i(\phi_e)$ we can compute the relationship between the cable tensions f_i and the torque $\widehat{\tau}_a$ delivered to the elbow joint. By defining the matrix J as:

$$J(\phi_e) = \frac{\partial h^T}{\partial \phi_e}(\phi_e) \tag{1.3}$$

where h represents the vector of cable extensions, the estimated assistive torque generated by bowden-cable transmission $\widehat{\tau}_a$ is expressed by the equation:

$$\widehat{\tau}_a = J(\phi_e)f \tag{1.4}$$

where f represents the vector of cable tensions.

The human arm dynamics, used for admittance controller, can be obtained by the Lagrangian formulation [41]:

$$\tau = \tau_h + \tau_a = \frac{2}{3} m l^2 \ddot{\phi}_e + b_e \dot{\phi}_e + m g l_c \sin \phi_e \tag{1.5}$$

where τ is the resulting torque of the human action τ_h and the assistive torque from the exosuit τ_a, while ϕ_e, $\dot{\phi}_e$ and $\ddot{\phi}_e$ denote the measured elbow angular position, velocity, and acceleration respectively; b_e is the viscous damping constant; and $g = 9.81\text{m/s}^2$ represents the gravity constant. The torque deriving from the human muscles τ_h can be obtained from the inverse dynamic model expressed by (1.5), i.e.,

$$\widehat{\tau_h} = \frac{2}{3} m l^2 \ddot{\phi}_e + b_e \dot{\phi}_e + m g l_c \sin \phi_e - \widehat{\tau_a} \tag{1.6}$$

where $\widehat{\tau_a}$ is the estimated assistive torque obtained from equation (1.4).

The parameters of equation 1.4 can be opportunely tuned on each individual subject following a set of simple known rules[42]: (1)The forearm mass m as 2.2% of the total body weight M, i.e., $m = 0.022M[\text{kg}]$; (2) The length l_c from the elbow joint to the center of gravity as 68.2% of the total forearm length l, i.e., $l_c = 0.682l[\text{m}]$; (3) The human elbow viscous damping coefficient b_e varies in a range of $0.4 - 2.5\text{Nm/(rad/s)}$.

The exosuit, which was used in the present work, has been conceived as a device to provide assistance to impaired people, in particular to stroke subjects who do not preserve enough residual voluntary capacity of motion to lift their elbow. Hence after the human torque $\widehat{\tau_h}$ has been estimated by the aforementioned model.

A successive block in the controller must generate a reference trajectory ϕ_e^d which the actuation must deliver to the human joint. In order to provide a smooth intervention of the actuation on the user an admittance controller has been used: the admittance controller has the role of changing the overall dynamics, increasing the transparency of the exosuit itself and decreasing the mechanical impedance of the human biomechanics. The result is an assistance which is gradually modulated and depends on the mutual interaction between the device and the wearer. The admittance control block can be defined as follows:

$$I_e^d \ddot{\phi}_e^d + b_e^d \dot{\phi}_e^d + K_e^d \sin \phi_e^d = \widehat{\tau_h} \tag{1.7}$$

where I_e^d, b_e^d, and K_e^d denotes the desired inertial, viscous damping and gravitational torque acting at the elbow joint, respectively, while and $\widehat{\tau_h}$ represents the estimated human torque obtained from equation (1.6). The gain of the admittance controller (I_e^d, b_e^d, and K_e^d) were chosen according to equation (1.8).

$$\begin{cases} I_e^d = \frac{2}{3} m l^2 \\ b_e^d = b_e \\ K_e^d = \alpha m g l_c \\ \alpha = \alpha_0 \tanh\left(\frac{\dot{\phi}_e}{\varepsilon_\alpha}\right) + \alpha_1 \end{cases} \tag{1.8}$$

where α_0 and α_1 are two constants experimentally chosen to bound the intervention of the assistance and ε_α denotes the sensitivity coefficient of the hyperbolic function $\tanh(.)$. The factor α increases with the measured joint velocity $\dot{\phi}_e$, meaning that the level of assistance is strictly dependent on the user's residual motion capacity: a high motion speed from the user (i.e. high motor ability) corresponds to a low assistive torque provided by the exosuit and viceversa, and the device is therefore able to gradually tune the assistive torque based on the a realtime estimation of the subject's capacity of motion.

1.2.2.2 Mid-level Controller: Adaptive Backlash Compensation

The purpose of the mid-level control layer is to compensate for the nonlinear backlash phenomenon typical of the bowden cable transmission. The desired angular motion ϕ_e^d from the admittance control block must be converted into a motion ϕ_a^d which is successively sent to the servomotor and delivered at the elbow joint. The mid-level controller is implemented with the purpose to specifically compensate for backlash phenomena. The relationship between the desired motion ϕ_e^d and the motion the actuation unit ϕ_a^d is defined adopting the Bouc-Wen hysteresis model [43], such that the desired elbow motion is a function of the actuator rotation and a term representing the backlash uncertainties:

$$\phi_e^d = \alpha_\phi \phi_a^d + D \rightarrow \beta \phi_e^d = \phi_a^d + \beta D \tag{1.9}$$

where α_ϕ represents the positive ratio of ϕ_e^d to ϕ_a^d; β is the inverse of α_ϕ; and D represents the model uncertainties due to the bowden sheath's configuration variations during operation.

The adaptive controller design uses a reference motion ϕ_e^r and sliding surface s as in:

$$\begin{cases} e = \phi_e - \phi_e^d \\ s = \lambda e + \int_0^t e d\tau \rightarrow \dot{s} = \lambda \dot{e} + e \\ \phi_e^r = \phi_e^d - \lambda \dot{e} \end{cases} \tag{1.10}$$

where e represents the tracking error between the desired elbow joint motion ϕ_e^d and the measured one ϕ_e; and λ is an arbitrarily positive constant. Since the elbow joint is supposed to follow a given trajectory ϕ_e^d, the desired actuator state ϕ_a^d can be chosen as:

$$\phi_a^d = \widehat{\beta} \left(\phi_e^r - \widehat{D_m} \tanh\left(\frac{s}{\varepsilon}\right)\right) - \kappa s \tag{1.11}$$

where $\widehat{\beta}$ and $\widehat{D_m}$ are the estimated value of β and D_m respectively (such notation will be used for all variables from now on); and κ, ε are positive constants.

Replacing ϕ_a^d from (1.11) to (1.9) leads to the dynamics of the sliding surface s as:

$$\beta \dot{s} + \kappa s = \widetilde{\beta} \tilde{\phi} - \beta \widetilde{D_m} \tanh\left(\frac{s}{\varepsilon}\right) - \beta \left(D_m \tanh\left(\frac{s}{\varepsilon}\right) - D\right) \tag{1.12}$$

where $\bar{\phi} = \phi_e^r - \widehat{D_m}\tanh\left(\frac{s}{\varepsilon}\right)$; $\widetilde{\beta} = \widehat{\beta} - \beta$ is the estimated error of β; and $\widetilde{D_m} = \widehat{D_m} - D_m$ is the estimated error of D_m.

Therefore, the adaptation law for backlash model parameters $\widehat{\beta}$ and $\widehat{D_m}$ is:

$$\begin{cases} \dot{\widehat{\beta}} = -\delta_1 \bar{\phi} s \\ \dot{\widehat{D_m}} = \delta_2 \beta \tanh\left(\frac{s}{\varepsilon}\right) s \end{cases} \tag{1.13}$$

where δ_1, δ_2 are positive adaptation gains. The initial values for $\widehat{\beta}$ and $\widehat{D_m}$ are set to be zero.

1.2.2.3 Low-level Controller: friction compensation and position control

The low level control layer is intended to drive the actuation stage by sending the input to the DC motor and to compensate for the nonlinear friction occurring because of the cable sliding along the bowden sheath. The friction continuously and unpredictably changes according to the curvature of the sheath which moves with the subject arm motion; if not compensated, the torque generated by the actuator is partly lost during operation. An adaptive algorithm compensates for the friction and controls the DC motor in tracking the desired trajectory ϕ_a^d. The actuator with the friction is modeled as follows:

$$J\ddot{\phi}_a + B\dot{\phi}_a + \tau_f = u \tag{1.14}$$

where J and B represent the inertia and damping coefficient of the actuation stage, τ_f the friction torque, and u is the control output to be sent to the DC motor. The dynamic parameters of the actuation stage comprising the DC motor and the bowden cable and the friction variability are unknown: the LuGre model for the dynamic friction compensation [44], allows to express τ_f as follows:

$$\tau_f = B_v\dot{\phi}_a + \tau_z\left(\phi_a, \dot{\phi}_a, z\right) \tag{1.15}$$

where z is a variable in the Lugre model; $B_v\phi_a$ represents the viscous friction; and $\tau_z\left(\phi_a, \dot{\phi}_a, z\right)$ represents the dynamic friction depending on z. Before designing the control signal u, we define the tracking error e_1, reference motion $\dot{x_a^r}$ and sliding surface s_1 for the actuator as:

$$\begin{cases} e_1 = \phi_a - \phi_a^d \\ s_1 = \dot{e_1} + \lambda_1 e_1 \\ \dot{\phi_a^r} = \dot{\phi_a^d} - \lambda_1 e_1 \end{cases} \tag{1.16}$$

where ϕ_a and ϕ_a^d denote the measured and desired rotation of the DC motor, respectively; and λ_1 is an arbitrary positive constant. The control signal u for the DC motor is designed as:

$$u = \widehat{J}\ddot{\phi}_a^r + \left(\widehat{B} + \widehat{B_v}\right)\dot{\phi}_a - \widehat{\tau_{zm}}\tanh\left(\frac{s_1}{\varepsilon_1}\right) - \kappa_1 s_1 \tag{1.17}$$

Table 1.2: Average Identified Control Model Parameters

Parameters	Values [Unit]
a, b, R	0.05[m], 0.10[m], 0.06[m]
m, l, l_c	1.55 ± 0.12[kg], 0.24 ± 0.03[m], 0.2 ± 0.02[m]
b_e	1.50[Nm/(rad/s)]
α_0, α_1, ε_α	0.5, 0.5, 0.1
λ, κ, ε, σ_1, σ_2	2, 10, 0.01, 2, 2
λ_1, κ_1, ε_1, σ_3, σ_4, σ_5	1.5, 5, 0.01, 1, 1, 1

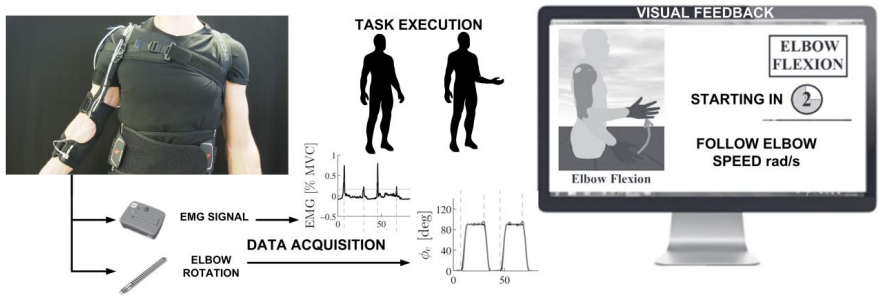

Figure 1.6: The experiment was run by instructing the subjects to replicate the movements of a virtual avatar on the screen trying to match the elbow speed. EMG and elbow flexion ϕ_e were acquired and post processed to compare the muscular activities.

where $\widehat{J}$ is the estimated value of J; $\widehat{B}$ and $\widehat{B_v}$ denote respectively the estimated values of B and B_v; $\widehat{\tau_{zm}}$ denotes the estimated value of τ_{zm}; and ε_1 and κ_1 are two positive constants. Substituting (1.15) and (1.17) to (1.14), and replacing $B_t = B + B_v$ result in the dynamics of the sliding surface s_1 as:

$$J\dot{s_1} + \kappa_1 s_1 = \widetilde{J}\ddot{\phi}_a^d + \widetilde{B}_t\dot{\phi}_a - \widetilde{\tau_{zm}}\tanh\left(\frac{s_1}{\varepsilon_1}\right) - \tau_{zm}\tanh\left(\frac{s_1}{\varepsilon_1}\right) - \tau_z\left(\phi_a, \dot{\phi}_a, z\right) \tag{1.18}$$

where $\widetilde{J} = \widehat{J} - J$ is the estimated error of J; $\widetilde{B}_t = \widehat{B}_t - B_t$ is the estimated error of B_t; and $\widetilde{\tau_{zm}} = \widehat{\tau_{zm}} - \tau_{zm}$ is the estimated error of τ_{zm}. Therefore, the unknown parameters $\widehat{J}$, $\widehat{B}_t$, and $\widehat{\tau_{zm}}$ are updated at each period by:

$$\begin{cases} \dot{\widehat{J}} = -\delta_3\ddot{\phi}_a^r s_1 \\ \dot{\widehat{B}}_t = -\delta_4\dot{\phi}_a s_1 \\ \dot{\widehat{\tau_{zm}}} = \delta_5\tanh\left(\frac{s_1}{\varepsilon_1}\right)s_1 \end{cases} \tag{1.19}$$

where δ_3, δ_4, and δ_5 are positive adaptation gains. Table 1.2 summarizes the identified control parameters averaged on three subjects.

1.2.3 Evaluation

The elbow exosuit was evaluated on three unimpaired subjects (Average age: 26.6±1.5), with the controller described above. The experiment aims at demonstrating that the proposed hierarchical controller is accurate, stable and provides a smooth intervention when assistance is requested by the users, modulating the amount of torque at the elbow depending on the capacity of motion of the subject and decreasing the muscular effort during load manipulation.

During the experiment the subjects were instructed to lift their forearm, following the motion of a virtual avatar on a screen (as shown in Figure 1.6) while holding a 1kg load in their left hand, in two distinct task phases: (1) performing 10 repetitive flexion/extension movements with and without assistance delivered by the exosuit to prove that the use of the proposed device/controller effectively decrease the muscular activity, helping the wearer to complete the task; (2) performing 10 repetitive flexion/extension movements at two different speeds ($\dot{\phi}_e^1 = 0.3\text{rad/s}$ and $\dot{\phi}_e^2 = 0.6\text{rad/s}$), to show that the intervention of the exosuit is based on the subject's capacity of motion. It is commonly accepted that kinematics in stroke subjects is dramatically jeopardized [45, 46] and a lower elbow speed is associated to a reduced voluntarily capacity of motion. For this reason, asking subjects to move at a lower and higher speed, implies that the proposed controller should interpret a lower speed as a reduced motion capacity and consequently increase the level of assistive torque respectively, as described in the section 1.2.2.1

Muscular effort was estimated from the Root Mean Square (RMS) of the EMG activity [47] of the main muscle involved in performing elbow flexion movements, i.e. the biceps brachii of the left arm. The raw EMG was acquired using Trigno wireless EMG sensors (Delsys Inc.) and was pre-processed in Matlab Simulink ® using a full-wave rectification, followed by a low-pass second-order Butterworth filter with a 8Hz cut-off frequency. The elbow joint angle ϕ_e was acquired during the experiment and used for control purposes using a resistive flex sensor (Spectrasymbol, USA). Data acquisition and motor control were performed using the Quanser Quarc® real-time workstation running at 1kHz refresh rate.

Results of the first task comparing the EMG activity of one subject with and without the assistance are depicted in Fig. 1.7a, showing a clear descrease in the amplitude of the EMG activity when the exosuit was assisting the motion. Analysis of the RMS value of the EMG signal, averaged over repetitions and subjects, is shown in Figure 1.7a. The latter shows an average drop in RMS of 48.3% between the non-assisted and assisted case. Figure 1.7b shows the estimated assistive torque, as computed from Equation 1.6 and the recorded EMG activity of a single flexion/extension task from one of the participants. This results in a trajectory profile as shown in Figure 1.7b, with a tracking error smaller than 0.3rad and a fast response time.

The second experiment examines the efficacy of the controller in adapting its contribution to the user's capacity of motion. The subjects performed the elbow movement at two different angular velocities ($\dot{\phi}_e^1 = 0.3\text{rad/s}$ and $\dot{\phi}_e^2 = 0.6\text{rad/s}$) and the exosuit modulates the degree of assistance, i.e. the assistive torque, based on

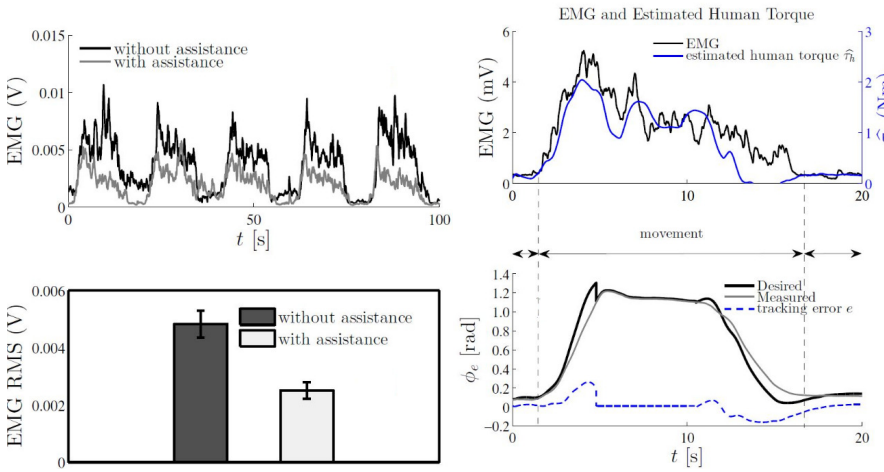

(a) (b)

Figure 1.7: Evaluation of the performance and assistance level of the proposed control paradigm. (a) The top plot shows the EMG amplitude comparison on a single subject with and without the exosuit's assistance,the bottom bar plot shows the mean and standard deviation of the RMS of the EMG activity, averaged over repetitions and subjects. (b) EMG and estimated human torque and trajectory tracking accuracy. The top plot shows the amplitude of the EMG signal (black) during a single repetition of a subject performing an elbow flexion/extension task and estimated human torque (gray) as computed from Equation 1.6. The bottom plot shows the trajectory tracking accuracy during a single flexion/extension task

the speed of the subjects. Fig. 1.8A-B shows the EMG activities and the delivered assistive torques $\widehat{\tau}_a$ respectively for one typical subject at the two execution speeds: it is observable that at lower speed (lower capacity of motion) the controller estimates a higher assistive torque than when the subject moves at the higher speed (which corresponds to a higher capacity of motion). The same result was observed for the whole group of subjects. An analysis of the EMG signals supports these results: Fig. 1.8.C shows that the mean RMS value of the EMG signal, averaged over subjects and trials, is lower at a lower speed of motion, confirming that the controller has adapted to the lower motor ability of the subjects by providing higher assistance.

1.2.4 Discussion

Despite the unquestionable advances achieved in the last 50 years in wearable assistive devices, current technologies are still far from being used on a daily basis. This is mostly due to their limitations in terms of portability, safety, ergonomics and, energy-wise, autonomy. Moreover, the cost of most of the developed exoskeleton make them prohibitive but for the most affluent users.

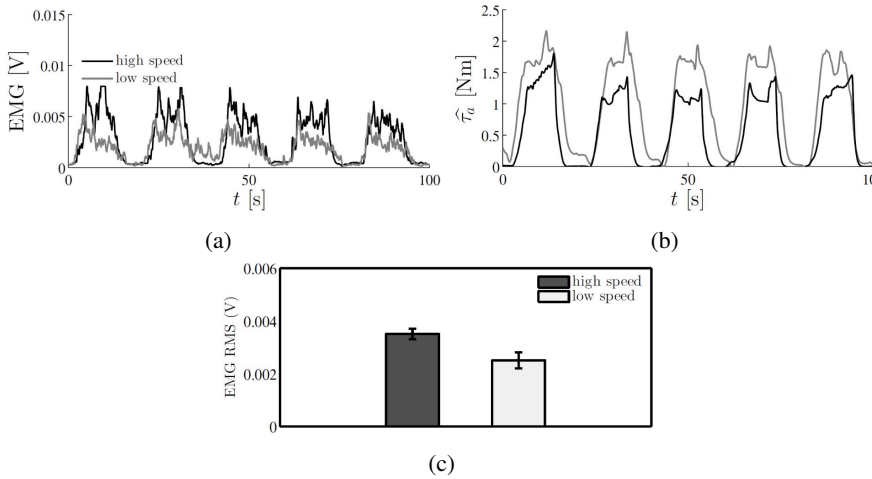

Figure 1.8: Evaluation of the effectiveness of the assistance modulation at different elbow speeds. (a) The amplitude of the EMG activities are shown when a single subject performed the elbow motions at two different velocities. When the subject moves slower (b) The assistive torques at a lower (light grey) and higher (dark grey) elbow speed motion. (c) Comparison of the EMG activity at low and high speed of movement with the proposed controller.

In this section we presented the design and testing of a soft wearable exosuit for assisting elbow movements and hand grasping. Using fabrics and bowden cables instead of traditional rigid transmissions would potentially result in cheaper devices, moreover making the device low-profile, lightweight, compliant and less restrictive to the wearer's motion. We based our design on a set of documented force and motion requirements and kept the weight and size of the actuators as low as possible. Finally, we introduced a novel, hierarchical control paradigm that exploits sensory data to adapt its model of the system, adapting to the wearer's retained motor capacity and compensating for the non-linear phenomena that make a simple linear control insufficient.

Despite having multiple advantages, exosuits rely on the wearer's skeletal structure to transmit compressive forces and are thus limited in the amount of assistance they can provide, especially if the wearer suffers from bone weakness caused by disuse osteporosis, a common co-morbodity of neuromuscular impairments [48]. This suggests that their effectiveness might be strongly dependent on the degree of retained motor ability of the patient. This point needs to be experimentally assessed: to the authors' knowledge, the only clinical criteria for the use of a soft wearable robot have been defined for the SEM Glove (Bioservo Ltd), which is recommended for patients with and Action Research Arm Test (ARAT) score between 10 and 35 and a Stroke Upper Limb Capacity Scale (SULCS) score of 4-7 [49]. We are confident that our glove could prove to be useful for a slightly larger population since it actuates both flexion and extension of the fingers, whilst the SEM glove only aids

gripping strength. No documented criteria, on the other side, exist for deciding the level of impairment that a soft elbow sleeve would be suitable for, thus tests with patients are of paramount importance for identifying the contribution of our technology.

In conclusion, whilst there is still a great need for improvement in the design, control and knowledge of their contribution, soft wearable devices for assitstance have the potential of becoming a valid and cost-effective solution for increasing independence and quality of life of patients suffering from motor disorders.

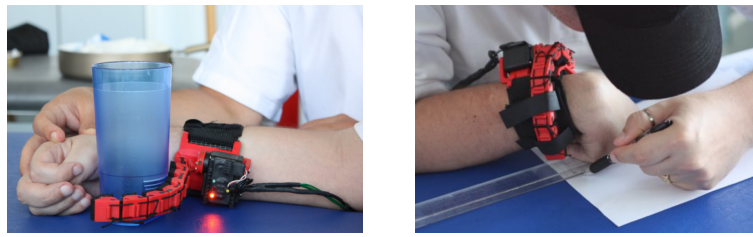

Figure 1.9: Working principle of the robotic extra finger. It cooperates with the paretic limb to compensate for hand grasp functionality (left), and it can be shaped into bracelet when not used (right).

1.3 Supernumerary Limbs

Long-term disabilities of the upper limb affects millions of stroke survivors [50]. More than 80% of individuals who experience severe hemiparesis after stroke cannot completely recover hand and arm use [51]. The improvement of the paretic hand functionality plays a key role in the functional recovery of stroke patients with a paretic upper limb [52, 53]. Different motor impairments can affect the hand both at motor execution and motor planning/learning level, including weakness of wrist/finger extensors, increased wrist/finger flexors tone and spasticity, co-contraction, impaired finger independence, poor coordination between grip and load forces, inefficient scaling of grip force and peak aperture, and delayed preparation, initiation, and termination of object grip [54]. In the last two decades, several rehabilitation teams have started integrating robotic-aided therapies in their rehabilitation projects. Such treatments represent a novel and promising approach in rehabilitation of the post-stroke paretic upper limb. The use of robotic devices in rehabilitation can provide high-intensity, repetitive, task-specific and interactive treatment of the impaired upper limb, and can serve as an objective and reliable means of monitoring patient progress [55, 56, 57]. Most of the proposed devices for hand and arm rehabilitation are designed to increase functional recovery in the first period after the stroke when, in some cases, biological restoring and plastic reorganization of the central nervous system take place [58]. However, even after extensive therapeutic interventions in acute rehabilitation, the probability of regaining functional use of the impaired hand is low [59]. For this reason, we recently started studying robotic devices for the compensation of hand function in chronic stroke patients, and in [60, 61, 62] we introduced a wearable robotic extra finger that can be used as an active compensatory tool for grasping objects.

The working principle of the proposed extra finger is rather simple and intuitive. The device can be worn on the paretic forearm by means of an elastic band, so that the robotic finger and the paretic hand can act like the two parts of a gripper working together to hold an object, see Fig. 1.9. This solution represents the minimum robotic complexity necessary to perform grasping tasks. To further improve its wearability, the finger can be shaped into bracelet when being not used. The user can control its flexion/extension through an EMG interface placed on the patient forehead [63] or

through wearable switches [64], as described in Section 1.3.2. In [65], we showed how the supernumerary finger can be used in activities of daily living (ADL) involving common bimanual tasks such as opening cans and jars with different closing systems and shapes. Sections 1.3.1 and 1.3.2 present the principles that can be used to design and control supernumerary limbs and, in particular, focus on the choices that were made for the Soft-SixthFinger. The reader can refer to Section 1.3.5 for details on the application and on the performance evaluation of the device.

1.3.1 Design and Actuation

Wearable assistive robotic devices used for clinical applications must meet specific human factors and performance criteria. The general guidelines which can be found in the literature include: durability, energy efficiency, low-encumbrance, ease of use, error tolerance, and configurability [66].

Two key characteristics for supernumerary limbs are the wearability and the acceptability for the users, and, in order to improve them, the design must satisfy a number of conditions related to ergonomics and functionality [67]. The specific indexes to be used and the human ergonomics strongly depend on the actual patient conditions and needs [68, 69]. Several experiments with patients, conducted in cooperation with a rehabilitation team, and reported in [62, 65, 63], led us to the development of the Soft-SixthFinger.

This supernumerary finger has been designed to be wearable, robust, and capable of adapting to different objects. In general, the robustness plays a twofold role: it makes the device capable of withstanding large impacts and other forces due to the unintended contact with the environment; it enables the robotic device to reliably grasp objects in presence of sensory uncertainty and unpredictable environment features. In previous works, robustness and soft interaction are achieved either by regulating the compliance of the robotic joints [70] or by tuning the intrinsic softness, acting on the passive characteristics of the robot bodyware [71, 72, 73]. The former approach is based on complex and bulky variable impedance actuators that are more suitable for other applications. Differently, our device is inspired by the latter approach in order to be simple, lightweight and compact. In particular, passive compliant joints and cable driven actuation guarantee robustness and safety during the interaction with the environment. These two characteristics not only assure that the device can endure collisions with hard objects and even strikes from a hammer without breaking into pieces, but also allow it to be highly adaptable to different object shapes, as it typically happens in underactuated and compliant hands [74]. In such types of robotic hands, in fact, transmission solutions that allow the motion of the other joints to continue after a contact occurs on a coupled link enable the device to passively adapt to objects using a reduced set of control parameters and in presence of uncertainties in sensing and actuation [75, 76].

As shown in Fig. 1.10, the Soft-SixthFinger is composed of two main parts: a flexible finger and a support base, coupled through a passive locking mechanism needed to switch between working and rest position (Fig. 1.9). The flexible finger is built with a modular structure. Each module consists of a rigid 3D printed

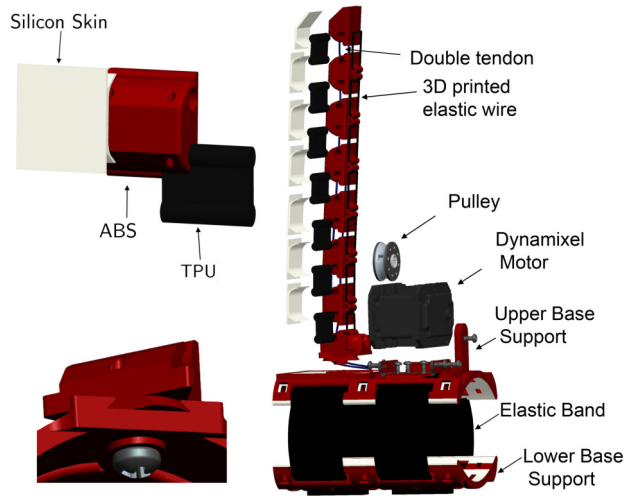

Figure 1.10: The CAD exploded view of a module (top left), the passive locking mechanism (bottom left), and the complete Soft-SixthFinger (right) with its tendon holes, support base, and actuator.

link made of ABS (Acrylonitrile Butadiene Styrene, ABSPlus, Stratasys, USA) and covered with a silicon skin, and a flexible 3D printed joint made of thermoplastic polyurethane (NinjaFlex®). We selected polyurethane for the flexible parts because the high elongation of this material allows for repeated movement and impact without wear or cracking, proving also an excellent vibration reduction. Reasons for adding passive elements are manifold, including storing elastic energy, avoiding tendon slackness and ensuring the uniqueness of the position of the extra-finger when not in contact with the object [77]. The modules are connected one to each other by sliding the thermoplastic polyurethane part inside the ABS one. This method allows to assemble the device in an easy way, without using any screw to combine the modules.

The device is developed by combining two different manufacturing processes: rapid prototyping 3D printing for the structure and molding for the silicon skin. The molding process shapes the raw material using a solid frame of a particular shape, called a pattern. We used 3D printed skeletons to hold the liquid silicon in the desired shape until it turned solid. We realized closed-top molds which are used for more complex part geometries. We pored the silicon mixture over the skeletons of the modules and used other mold's parts to constrain the liquid silicon to achieve the desired geometry and shape of the skin. Metal tubes were inserted into the module holes so to avoid silicon to fill the tendon holes. The silicon used is Fast Rubber FR-18 which is bi-component curing at room temperature. The mixing ratio of components is 100 g of base per 5 g of catalyst. It has viscosity of 30 $Pa{\cdot}s$ and the final hardness is $17{\pm}2$ *shore A*. The silicon skin on the rigid links aiming to increase the friction at the possible contact areas.

The support base of the finger has been designed to guarantee a firm grip on the arm of the user and the wearability of the entire device. It consists of two parts coupled with velcro strips to facilitate the wearing process and assure the adaptation to different arm sizes. The upper part contains the actuation system of the Soft-SixthFinger that consists of a single actuator and two tendons running in parallel through the modules of the finger. The cables (polyethylene dyneema fiber, Japan) run through the finger and are attached on one side to the fingertip and on the other one to a pulley rigidly connected to the actuator shaft. When the motor is actuated, the tendon wires are wound on the pulley reducing the length of the wire and thus flexing the finger. As the motor is rotated in the opposite direction, the extension of the finger is achieved thanks to the elastic force stored in the flexible joints. Currently, we are using as actuator a Dynamixel MX-28T (Robotis, South Korea) driven by an ArbotiX-M Robocontroller [78].

1.3.2 Control

One of the major challenges in the development of extra limbs, lies in finding suitable control interfaces for the integration of the robotic devices with the human. The choice of the control strategy to adopt, strictly depends on the design of the supernumerary limb and on its purpose. In [79], authors present a control algorithm enabling a human hand, augmented with two robotic fingers, to share the task load together and adapt to diverse task conditions. Postural synergies were found for the seven-fingered hand comprised of two robotic fingers and five human fingers through the analysis of measured data from grasping experiments. Prattichizzo *et al*. in [60] describe a mapping algorithm able to transfer to an arbitrary number of robotic extra-fingers the motion of the human hand. The algorithm is based on the method proposed in [80], in which the mapping procedure was developed to reproduce human hand postural synergies on robotic hands with a dissimilar kinematics. In [60], this procedure is extended to the case of a human hand augmented with robotic extra-fingers, introducing an interesting and, to the best of our knowledge, still not very exploited framework, in which the human part and the robotic one share a common workspace. The human hand and the supernumerary extra fingers define a higher level kinematic structure that we referred to as *augmented hand*. The mapping algorithm is based on the definition of a virtual object obtained as a function of a set of reference points placed on the augmented hand, and allows to move the extra-fingers according to the human hand motions, without requiring any explicit command from the user. This type of control strategy was successfully applied to a fully actuated robotic finger used by an healthy human, and was found to be useful in tasks that are typically rather difficult, such as grasping a large object or holding a bottle and unscrewing its cap with the same hand, see Fig. 1.11.

Both control approaches presented in [79, 60] used an instrumented glove to track the human hand. However, in applications where the coordination between the human hand and the robotic extra limb is not a feasible solution, e.g., when extra-limbs are used for patients that are not able to control their hand motion due to an upper limb paralysis, alternative solutions must be explored. A possibility is to use

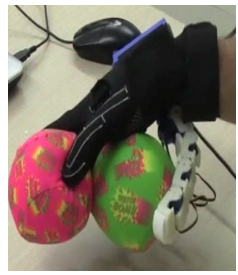


Figure 1.11: Fully actuated extra finger to enhance the capabilities of an healthy human hand. Left: grasping multiple objects in one augmented hand (ulnar grasp). Right: grasp of a big object (anatomically impossible grasp).

wearable control interfaces designed to be as intuitive and easy-to-use as possible. These features become paramount, for example, in chronic stroke patients that may also be affected by some cognitive deficit, possibly limiting their compliance during a demanding learning phase.

Next subsections describe two of the most suitable interfaces that were used to control the Soft-SixthFinger: the wearable cutaneous device called hRing and the EMG interface called frontalis muscle cap.

1.3.3 The hRing

All the above mentioned works for the design of novel supernumerary limbs have shown incredibly promising results, re-enabling impaired users to grasp objects they would not be able to grasp otherwise. Despite this, most of them do not provide any information about the forces exerted by the supernumerary limb on the environment, which is known to be useful [81, 82, 83]. Often this is not necessary, as operators use their own bodies to counterbalance the forces exerted by the supernumerary limb. For example, in Fig. 1.9, the patient through his own hand can feel the force applied by the robotic finger through the object [65]. However, this is not always the case. In fact, many post-stroke patients suffer from tactile anesthesia, or anaphia [84, 85], in the hand contralateral to the stroke, which is the one that should provide force information about the supernumerary limb. For this reason, there have been attempts to restore the sense of touch in patients affected by this deficit. In this respect, the group at the University of Siena proposed a wearable cutaneous interface with the purpose of relying information about the force exerted by the robotic finger. It can be worn on the proximal finger phalanx of the healthy hand and it is called hRing.

A prototype of the hRing is shown in Fig. 1.12a, and Hussain *et al*. [65] tested it together with the Soft-SixthFinger described in Section 1.3.1. It consists of two servo motors, a vibrotactile motor, two pairs of push buttons, and a belt. The servo motors move the belt in contact with the user's finger skin. When the motors spin in opposite directions, the belt presses into the user's finger, while when the motors spin in the same direction, the belt applies a shear force to the skin. The device structure is sym-

(a) (b)

Figure 1.12: Possible interfaces for supernumerary limbs. (a) The hRing: It consists of two servo motors, a vibrotactile motor, two pairs of push buttons, and a belt. (b) The frontalis muscle cap: It is an EMG interface where electrodes are placed inside the cap at front side to be positioned on the patients forehead. The acquisition board and a vibrating motor are placed in a box on the back of the cap. An LED board at the base of robotic finger shows the activation of trigger signal and status of device.

metrical and each side features two push buttons, enabling the hRing to be used both on the left and on the right hand. Through the moving belt, the hRing is able to provide normal and shear stimuli at the fingertip. Through the vibrotactile motor, it can provide vibrotactile transients information, such as the making and breaking contact with the grasped object. Moreover, featuring two push buttons, users can close the robotic finger and increase the grasping force (blue button in Fig. 1.12a), and reduce the grasping force and open the robotic finger (yellow button in Fig. 1.12a).

Two chronic stroke patients took part to the experimental evaluation of this interface for supernumerary limbs [64]. Each patient used the Soft-SixthFinger and the hRing for bimanual tasks, such as unscrewing a cap of a tomato jar, opening a popcorn bag, or opening a can of beans. Both patients were able to carry out several ADL bimanual tasks that would have not been possible without the supernumerary robotic system. Moreover, they both appreciated the haptic feedback. The demonstration of this integrated system (Soft-SixthFinger and hRing) was awarded with the Best Demonstration Award at the 2016 IEEE Haptics Symposium in Philadelphia, USA. The same haptic device was also used for other applications, not paired with a supernumerary limb. Pacchierotti et al. [86], for example, used it to provide haptic feedback in a virtual environment. The authors showed that providing tactile feedback through the device improved the performance and perceived effectiveness of the virtual interaction task of 20% and 47% with respect to not providing any force feedback, respectively.

1.3.4 The frontalis muscle cap

The use of the hRing to control the motion of a robotic finger requires the involvement of the healthy hand. To cope with this issue, we proposed the frontalis muscle cap [65], an EMG based wireless interface which maintains the principle of simplic-

Table 1.3: Motion control of soft sixth finger using trigger signal.

Trigger signal	**Associated action**
single trigger	move/stop
double trigger	change direction

ity of a switch without interrupting the patient activities and without the involvement of the healthy hand during task execution.

Several EMG interfaces have been already successfully adopted for the control of prosthesis [87] and exoskeletons [88]. The EMG electrodes are usually placed either in the muscles coupled with the robot (exoskeleton) or in muscles where amputees still have the phantom of functions and hence they are able to generate a repeatable EMG pattern corresponding to each of the functions (prosthesis). For chronic stroke patients it is generally difficult to generate repeatable EMG patterns in their paretic upper limb due to the weakness in muscle contraction control. For this reason, we coupled the flexion/extension motion of the robotic device with the contraction of the frontalis muscle. The user can contract this muscle by moving the eyebrows upwards. This muscle is always spared in case of a motor stroke either of the left or of the right hemisphere, due to its bilateral cortical representation [89].

The frontalis muscle cap is a wearable wireless EMG interface where electrodes, acquisition and signal conditioning boards, as well as a vibration motor to provide haptic feedback are embedded in a cap, see Fig. **??**. This solution allows the patients to autonomously wear the interface using only their healthy hand. The vibration motor provides the feedback about the robotic finger status in terms of contact/no contact with the grasped object and in terms of force exerted by the device. The acquired EMG signal is sampled at 1 kHz (double EMG band) to avoid aliasing and a wireless communication is realized by a pair of Xbee modules (Series 1). The transmitter is embedded in the frontalis muscle cap while the receiver is placed on the actuator controller unit (specifications of the EMG acquisition board are summarized in Table 1.4). The reference values of received EMG signals were normalized using maximum voluntary contraction (MVC) technique [90]. This solution avoids the problems related to the high influence of detection condition on EMG signal amplitude. In fact, amplitude can greatly vary between electrode sites, subjects, and even day to day measures of the same muscle site. We implemented an auto-tuning procedure based on the MVC in order to better match the user-dependent nature of the EMG signal. The motion of the compensatory robotic device is controlled by using a finite state machine based on a trigger signal generated by using the hRing or the frontalis muscle cap. When using the EMG control interface, the trigger signal is obtained by using a single-threshold value defined as the 50% of the MVC, a level that was repeatable and sustainable for the subject without producing undue fatigue during the use of the device [65]. The state machine works under the simple control strategy presented in Table 1.3.

1.3.5 Evaluation

This section explains two aspects of the evaluation of a supernumerary finger. On one side (Section 1.3.6), there is the need of assessing the characteristics of the robotic device from a quantitative point of view using standard indexes devised for robotic grippers (Table 1.4), and from a qualitative point of view, evaluating its shape adaptability to a standard database of objects [91]. On the other side (Section 1.3.7), it is important to check whether the device works as expected when used by patients.

1.3.6 Performance evaluation

The performances of the Soft-SixthFinger were evaluated through a subset of the tests proposed in [92]. In particular, we measured the maximum fingertip force, the maximum payload and maximum horizontal grasp resistive force. The results of the experiments are summarized in Table 1.4. The maximum fingertip force of the device was recorded while fixing its support base on a table with the finger perpendicular to the table surface. The initial configuration of the finger was fully extended and it was commanded to close at the maximum torque. The hook of a dynamometer (Vernier, USA) was rigidly coupled with the fingertip of the device so to measure the force in the vertical direction. The maximum horizontal grasp resistive force was measured by grasping an object (diameter=65 mm, weight=400 g) with the robotic device and the arm while resting the arm on the table. The object was slowly pulled horizontally w.r.t the table surface. To check the maximum payload, the operator's arm was stabilized on a table while grasping a cylindrical object (diameter=65 mm, weight=400 g) with the aid of the Soft-SixthFinger driven at the maximum actuator's torque. The grasped object was slowly pushed down using the dynamometer's bumper. The maximum pushing force was recorded when the object started to slip. The maximum payload of the device is the sum of the weight of the grasped object and the load due to the pushing force.

In order to prove the grasping ability of the device and its shape adaptability to different objects, we used a subset of the objects of the YCB grasping toolkit [91]. This toolkit is intended to be used to facilitate benchmarking in prosthetic design, rehabilitation research, and robotic manipulation. The objects in the set are designed to cover a wide range of aspects of the manipulation problem. It includes objects of daily life with different shapes, sizes, textures, weight and rigidity. In general, grasp success is greatly affected by the ability of the robotic device to adapt to the shape of the object and the environment in response to contact forces. This adaptation increases the contact area and thereby the robustness of the grasp. In literature, the improvements on grasping of unknown object obtained through shape adaptation are well known [76, 93, 94, 72]. We tested the device with different objects to evaluate how the robotic finger can adapt to the shape of the objects to realize a stable enveloping grasp. The tests were performed by a healthy subject wearing the device. This assured to evaluate only shape adaptation of the Soft-SixthFinger, avoiding possible grasp failures which could occur due to the low residual mobility of patients'

Table 1.4: Technical details of the complete system

Dimensions	
Module	$20 \times 31 \times 12$ mm^3
Total length of finger (on arm)	180 mm
Support base	$110 \times 63 \times 3.5$ mm^3
Actuator control unit box	$71 \times 71 \times 45$ mm^3
Weights	
Module	4 g
Actuator control unit box	146 g
Actuator	
Max. torque	3.1 Nm @ 12 V
Pulley radius	8 mm
Max. current	1.4 A @ 12 V
Continuous operating time	3.5 h @stall torque
Max. operating angles	300 deg, endless turn
Max. non-loaded velocity	684 deg/sec
The SSF performances	
Max. Force at fingertip	40 N
Max. payload	2.4 kg
Max. horizontal resistive force	13 N @ dia=65 mm
Total: finger + support base	180 g
Diameter smallest graspable obj.	14 mm
Motion Control	
Single trigger	Move/stop
Double trigger	Change direction
Specifications of EMG Acquisition Board	
EMG acquisition box dimensions	$35 \times 31 \times 45$ mm^3
EMG acquisition box weight	46 g
Principle	Differential voltage
Number of electrodes	3
Bandwidth	$10 - 400$ Hz
Gain	1000
Input Impedance	100 GΩ
CMRR	110 dB
Operating voltage	Vcc = 3.3 V

Figure 1.13: Example of a bi-manual tasks (*left*) and a task of Frenchay Arm Test (*right*), performed by patients using two different control interfaces: the hRing (*left*) and the frontalis muscle cap (*right*), are shown.

arms. The finger was able to adapt itself to the shape of the grasped objects due to its intrinsic compliance [65].

1.3.7 Tests with chronic stroke patients

We tested the proposed device with six chronic stroke patients (five males, one female, age $40-62$) to see how it can be used for hand grasping compensation in subjects showing a residual mobility of the arm. For being included in the experimental phase, patients had to score ≤ 2 when their motor function was tested with the National Institute of Health Stroke Scale (NIHSS) [95], item 5 "paretic arm". Moreover, the patients had to show the following characteristics: normal consciousness (NIHSS, item 1a, 1b, 1c = 0), absence of conjugate eyes deviation (NIHSS, item $2 = 0$), absence of complete hemianopia (NIHSS, item $3 \leq 1$), absence of ataxia (NIHSS, item $7 = 0$), absence of completely sensory loss (NIHSS, item $8 \leq 1$), absence of aphasia (NIHSS, item $9 = 0$), absence of profound extinction and inattention (NIHSS, item $11 \leq 1$). The goal of the tests was to verify how quickly the patients can learn to use the device and its control interface. We performed qualitative tests composed of the Frenchay Arm Test [96], and some ADL bi-manual tasks, where the paretic limb and the robotic finger worked together to constrain the motion of the object while the healthy hand manipulated it (e.g., constrain the motion of a jar while unscrewing its cap). Fig. 1.13 shows two examples of tasks performed by the patients, whereas detailed results are presented in [65, 64].

1.3.8 Discussion

In this part of the chapter, we presented the newly introduced *framework* of supernumerary robotic limbs and shared our experience regarding the development of supernumerary robotic fingers that can be used for augmenting and compensating the human manipulation abilities. In particular, the new generation of robotic fingers can be used by the stroke patients to recover their missing grasping abilities and by healthy subjects to enhance their manipulation capabilities. For people with paretic

upper limb, most of the attention of the community has been focused on exoskeletons [97] which are very difficult to use specially in chronic stage because of their limitation in accommodating the subjects anatomical variations due to impairment. Moreover, the poor wearability, in terms of weight and size, make them difficult to use in ADL. One of the biggest challenge of rehabilitation and assistive engineering is to develop technology to practice intense movement training at home [98]. The creation of a functional grasp by means of the supernumerary fingers enables patients to execute task-oriented grasp and release exercises and practice intensively using repetitive movements. Supernumerary robotic fingers can increase patients' performances, with a focus on objects manipulation, thereby improving their independence in ADL, and simultaneously decreasing erroneous compensatory motor strategies for solving everyday tasks. The idea of wearable supernumerary limbs as assistive devices is different in nature than other approaches used in rehabilitation and assistive robotics. Supernumerary limbs will provide novel opportunities to recover missing abilities, resulting in improvements of patients' quality of life. One of the more important aspects that has to be taken into account when designing supernumerary limbs is their close interaction with the human body. For this reason the design guiding principles are safety, wearability, ergonomics and user comfort. Although, until now the supernumerary robotic fingers are mainly being used for grasping compensation but there is a good expectation in using these devices to rehabilitate at least the arm.

Moreover, we also believe that extra-fingers can play a role even in hand rehabilitation. Patients with hemiparesis often have limited functionality in the left or right hand. The standard therapeutic approach requires the patient to attempt to make use of the weak hand even though it is not functionally capable, which can result in feelings of frustration. The aim is to provide patients with a sense of purpose and accomplishment during ADL training, even during the early phase of treatment when the task can only be partially completed. We hope that the proposed devices can facilitate therapist-guided ADL training and encourage patients to continue exercising the affected limb. From the neuroscientific point of view, the development of this type of devices opens a series of interesting questions on how the supernumerary limbs are perceived by human cognitive system that needs to be investigated.For example, Hoyet *et al.* [99] measured humans' sense of ownership of a six-fingers hand avatar controlled in a virtual reality scenario. Participants responded positively to the possibility of controlling the six-fingers hand, despite the structural difference with respect to their own hand. In this respect, we are interested in evaluating the sense of ownership of our extra finger.

Acknowledgment

The research has received founding from European Unions Horizon 2020 Research and Innovation Programme, Grant Agreement No. 688857 (SoftPro) and from the European Union Seventh Framework Programme FP7/2007- 2013, Grant Agreement No. 601165 (WEARHAP).

Bibliography

[1] G. A. Pratt and M. M. Williamson, "Series elastic actuators," in *IEEE/RSJ Int. Conf. Intell. Robot. Syst. 'Human Robot Interact. Coop. Robot.*, vol. 1, pp. 399–406, IEEE Comput. Soc. Press, 1995.

[2] E. J. Rouse, L. M. Mooney, and H. M. Herr, "Clutchable series-elastic actuator: Implications for prosthetic knee design," *Int. J. Rob. Res.*, vol. 33, pp. 1611–1625, 2014.

[3] T. Noritsugu, H. Yamamoto, D. Sasakil, and M. Takaiwa, "Wearable power assist device for hand grasping using pneumatic artificial rubber muscle," *SICE 2004 Annu. Conf.*, vol. 1, pp. 420–425, 2004.

[4] G. Aguirre-Ollinger, J. E. Colgate, M. A. Peshkin, and A. Goswami, "Active-impedance control of a lower-limb assistive exoskeleton," in *2007 IEEE 10th International Conference on Rehabilitation Robotics*, pp. 188–195, June 2007.

[5] H. Herr, "Exoskeletons and orthoses: classification, design challenges and future directions.," *J. Neuroeng. Rehabil.*, vol. 6, p. 21, 2009.

[6] N. Karavas, A. Ajoudani, N. Tsagarakis, J. Saglia, A. Bicchi, and D. Caldwell, "Tele-impedance based assistive control for a compliant knee exoskeleton," *Robotics and Autonomous Systems*, vol. 73, pp. 78–90, 2015.

[7] A. T. Asbeck, S. M. M. De Rossi, K. G. Holt, and C. J. Walsh, "A biologically inspired soft exosuit for walking assistance," *Int. J. Rob. Res.*, vol. 34, no. 6, pp. 744–762, 2015.

[8] F. Panizzolo, I. Galiana, A. T. Asbeck, C. Siviy, K. Schmidt, K. G. Holt, and C. J. Walsh, "A biologically-inspired multi-joint soft exosuit that can reduce the energy cost of loaded walking," *J. Neuroeng. Rehabil.*, vol. submitted, p. 43, jan 2016.

[9] B. T. Quinlivan, L. Sangjun, P. Malcolm, D. M. Rossi, M. Grimmer, C. Siviy, and C. J. Walsh, "Assistance magnitude vs. metabolic cost reductions for a tethered multiarticular soft exosuit," *Sci. Robot.*, vol. 2, no. 2, pp. 1–17, 2016.

[10] H. In, B. B. Kang, M. Sin, and K. J. Cho, "Exo-glove: A wearable robot for the hand with a soft tendon routing system," *IEEE Robotics Automation Magazine*, vol. 22, pp. 97–105, March 2015.

[11] D. W. Robinson, *Design and analysis of series elasticity in closed-loop actuator force control*. PhD thesis, Massachusetts Institute of Technology, 2000.

[12] A. T. Asbeck, S. M. M. De Rossi, I. Galiana, Y. Ding, and C. J. Walsh, "Stronger, smarter, softer: Next-generation wearable robots," *IEEE Robot. Autom. Mag.*, vol. 21, pp. 22–33, dec 2014.

[13] S. M. M. D. Rossi, J. Bae, K. E. O. Donnell, K. L. Hendron, K. G. Holt, T. Ellis, and C. J. Walsh, "Gait improvements in stroke patients with a soft exosuit," *Proc. Gait Clin. Mov. Anal. Soc. Meet.*, pp. 2–3, 2015.

[14] M. Ding, J. Ueda, and T. Ogasawara, "Pinpointed muscle force control using a power-assisting device: System configuration and experiment," in *Proc. 2nd Bienn. IEEE/RAS-EMBS Int. Conf. Biomed. Robot. Biomechatronics, BioRob 2008*, pp. 181–186, IEEE, oct 2008.

[15] J. Ueda, M. Hyderabadwala, V. Krishnamoorthy, and M. Shinohara, "Motor task planning for neuromuscular function tests using an individual muscle control technique," in *IEEE Int. Conf. Rehabil. Robot.*, pp. 133–138, IEEE, jun 2009.

[16] S. W. Lee, K. A. Landers, and H.-S. Park, "Development of a biomimetic hand exotendon device (biomhed) for restoration of functional hand movement post-stroke," *IEEE Transactions on Neural Systems and Rehabilitation Engineering*, vol. 22, no. 4, pp. 886–898, 2014.

[17] H. In and K.-j. Cho, "Exo-Glove : Soft wearable robot for the hand using soft tendon routing system," *IEEE Robot. Autom.*, vol. 22, no. March 2015, pp. 97–105, 2015.

[18] T. Nef, M. Guidali, and R. Riener, "ARMin III arm therapy exoskeleton with an ergonomic shoulder actuation," *Appl. Bionics Biomech.*, vol. 6, pp. 127–142, jul 2009.

[19] C. Carignan, J. Tang, and S. Roderick, "Development of an exoskeleton haptic interface for virtual task training," in *IEEE/RSJ Int. Conf. Intell. Robot. Syst. IROS*, pp. 3697–3702, IEEE, oct 2009.

[20] Y. Ren, H. S. Park, and L. Q. Zhang, "Developing a whole-arm exoskeleton robot with hand opening and closing mechanism for upper limb stroke rehabilitation," in *IEEE Int. Conf. Rehabil. Robot. ICORR*, pp. 761–765, IEEE, jun 2009.

[21] S. J. Ball, I. E. Brown, and S. H. Scott, "MEDARM: A rehabilitation robot with 5DOF at the shoulder complex," in *IEEE/ASME Int. Conf. Adv. Intell. Mechatronics, AIM*, pp. 1–6, IEEE, 2007.

[22] H. S. Lo and S. Q. Xie, "Exoskeleton robots for upper-limb rehabilitation: State of the art and future prospects," *Med. Eng. Phys.*, vol. 34, pp. 261–268, apr 2012.

[23] K. Kiguchi, M. H. Rahman, M. Sasaki, and K. Teramoto, "Development of a 3DOF mobile exoskeleton robot for human upper-limb motion assist," *Rob. Auton. Syst.*, vol. 56, pp. 678–691, aug 2008.

[24] J. C. Perry, J. Rosen, and S. Burns, "Upper-limb powered exoskeleton design," *IEEE/ASME Trans. Mechatronics*, vol. 12, no. 4, pp. 408–417, 2007.

[25] S. Ueki, Y. Nishimoto, M. Abe, H. Kawasaki, S. Ito, Y. Ishigure, J. Mizumoto, and T. Ojika, "Development of virtual reality exercise of hand motion assist robot for rehabilitation therapy by patient self-motion control.," *Conf. Proc. IEEE Eng. Med. Biol. Soc.*, vol. 2008, pp. 4282–5, jan 2008.

[26] E. Carmeli, S. Peleg, G. Bartur, E. Elbo, and J. J. Vatine, "HandTutorTM enhanced hand rehabilitation after stroke - a pilot study," *Physiother. Res. Int.*, vol. 16, pp. 191–200, dec 2011.

[27] A. Chiri, N. Vitiello, F. Giovacchini, S. Roccella, F. Vecchi, and M. C. Carrozza, "Mechatronic design and characterization of the index finger module of a hand exoskeleton for post-stroke rehabilitation," *IEEE/ASME Trans. Mechatronics*, vol. 17, pp. 884–894, oct 2012.

[28] N. Jarrassé and G. Morel, "Connecting a human limb to an exoskeleton," *IEEE Trans. Robot.*, vol. 28, pp. 697–709, jun 2012.

[29] N. Jarrassé and G. Morel, "A formal method for avoiding hyperstaticity when connecting an exoskeleton to a human member," in *Proc. - IEEE Int. Conf. Robot. Autom.*, pp. 1188–1195, 2010.

[30] A. Stienen, E. Hekman, F. C. T. van der Helm, H. van der Kooij, and H. Stienen, A.H.A.; Hekman, E.E.G. ; van der Helm, F.C.T. ; van der Kooij, "Self-Aligning Exoskeleton Axes Through Decoupling of Joint Rotations and Translations," *IEEE Trans. Robot*, vol. 25, no. 3, pp. 628–633, 2009.

[31] M. Fontana, A. Dettori, F. Salsedo, and M. Bergamasco, "Mechanical design of a novel hand exoskeleton for accurate force displaying," in *Proc. - IEEE Int. Conf. Robot. Autom.*, pp. 1704–1709, 2009.

[32] K. Toya, T. Miyagawa, and Y. Kubota, "Power-Assist Glove Operated by Predicting the Grasping Mode," *J. Syst. Des. Dyn.*, vol. 5, no. 1, pp. 94–108, 2011.

[33] Y. Kadowaki, T. Noritsugu, M. Takaiwa, D. Sasaki, and M. Kato, "Development of soft power-assist glove and control based on human intent," *J. Robot. Mechatronics*, vol. 23, no. 2, pp. 281–291, 2011.

[34] P. Polygerinos, Z. Wang, K. C. Galloway, R. J. Wood, and C. J. Walsh, "Soft robotic glove for combined assistance and at-home rehabilitation," *Rob. Auton. Syst.*, vol. 73, pp. 135–143, 2015.

[35] H. Kobayashi and K. Hiramatsu, "Development of muscle suit for upper limb," in *IEEE Int. Conf. Robot. Autom. 2004. Proceedings. ICRA '04. 2004*, vol. 3, pp. 3–8, IEEE, 2004.

[36] A. T. Asbeck, R. J. Dyer, A. F. Larusson, and C. J. Walsh, "Biologically-inspired soft exosuit," in *IEEE Int. Conf. Rehabil. Robot.*, (Seattle, WA), pp. 1–8, 2013.

[37] A. T. Asbeck, K. Schmidt, and C. J. Walsh, "Soft exosuit for hip assistance," *Rob. Auton. Syst.*, vol. 73, pp. 102–110, 2015.

[38] H. In, H. Lee, U. Jeong, B. B. Kang, and K.-j. Cho, "Feasibility study of a slack enabling actuator for actuating tendon-driven soft wearable robot without pretension," in *Icra*, (Seattle, WA), pp. 1229–1234, 2015.

[39] L.-W. Tsai, *Robot Analysis and Design*. New York, NY, USA: John Wiley & Sons, Inc., 1999.

[40] R. M. Murray, Z. Li, and S. S. Sastry, *A Mathematical Introduction to Robotic Manipulation*, vol. 29. Boca Raton, Florida: CRC Press, 1994.

[41] K. Kong and M. Tomizuka, "Control of exoskeletons inspired by fictitious gain in human model," *IEEE/ASME Transactions on Mechatronics*, vol. 14, pp. 689–698, Dec 2009.

[42] M. B. Weinger, M. E. Wiklund, and D. J. Gardner-Bonneau, *Handbook of Human Factors in Medical Device Design*. 2010.

[43] F. Ikhouane and J. Rodellar, *Systems with hysteresis: analysis, identification and control using the Bouc-Wen model*. John Wiley & Sons, 2007.

[44] H. Olsson, K. strm, C. C. de Wit, M. Gfvert, and P. Lischinsky, "Friction models and friction compensation," *European Journal of Control*, vol. 4, no. 3, pp. 176 – 195, 1998.

[45] M. C. Cirstea, "Compensatory strategies for reaching in stroke," *Brain*, vol. 123, no. 5, pp. 940–953, 2000.

[46] A. Berardelli, M. Hallett, J. C. Rothwell, R. Agostino, M. Manfredi, P. D. Thompson, and C. D. Marsden, "Single-joint rapid arm movements in normal subjects and in patients with motor disorders.," *Brain*, vol. 119, pp. 661–674, 1996.

[47] R. E. Challis and R. I. Kitney, "Biomedical signal processing (in four parts). Part 1. Time-domain methods," *Med. Biol. Eng. Comput.*, vol. 28, no. 6, pp. 509–524, 1990.

[48] S. Takata and N. Yasui, "Disuse osteoporosis.," *J. Med. Invest.*, vol. 48, no. 3-4, pp. 147–56, 2001.

[49] M. Nilsson, A. F. Westerberg, and C. Wadell, "Grip strengthening glove to improve hand function in patients with neuromuscular disorders: A feasibility study," *J. Neuroeng. Rehabil.*, 2013.

[50] A. S. Go, D. Mozaffarian, V. L. Roger, E. J. Benjamin, J. D. Berry, M. J. Blaha, S. Dai, E. S. Ford, C. S. Fox, S. Franco, *et al.*, "Heart disease and stroke statistics–2014 update: a report from the american heart association.," *Circulation*, vol. 129, no. 3, p. e28, 2014.

[51] H. Nakayama, H. S. Jorgensen, H. O. Raaschou, and T. S. Olsen, "Compensation in recovery of upper extremity function after stroke: the copenhagen stroke study," *Archives of physical medicine and rehabilitation*, vol. 75, no. 8, pp. 852–857, 1994.

[52] G. Kwakkel and B. Kollen, "Predicting improvement in the upper paretic limb after stroke: a longitudinal prospective study," *Restorative neurology and neuroscience*, vol. 25, no. 5, pp. 453–460, 2007.

[53] I. Faria-Fortini, S. M. Michaelsen, J. G. Cassiano, and L. F. Teixeira-Salmela, "Upper extremity function in stroke subjects: relationships between the international classification of functioning, disability, and health domains," *Journal of Hand Therapy*, vol. 24, no. 3, pp. 257–265, 2011.

[54] S. Balasubramanian, J. Klein, and E. Burdet, "Robot-assisted rehabilitation of hand function," *Current opinion in neurology*, vol. 23, no. 6, pp. 661–670, 2010.

[55] B. T. Volpe, H. I. Krebs, and N. Hogan, "Is robot-aided sensorimotor training in stroke rehabilitation a realistic option?," *Current opinion in neurology*, vol. 14, no. 6, pp. 745–752, 2001.

[56] S. Masiero, A. Celia, G. Rosati, and M. Armani, "Robotic-assisted rehabilitation of the upper limb after acute stroke," *Archives of physical medicine and rehabilitation*, vol. 88, no. 2, pp. 142–149, 2007.

[57] A. Chiri, N. Vitiello, F. Giovacchini, S. Roccella, F. Vecchi, and M. C. Carrozza, "Mechatronic design and characterization of the index finger module of a hand exoskeleton for post-stroke rehabilitation," *Mechatronics, IEEE/ASME Transactions on*, vol. 17, no. 5, pp. 884–894, 2012.

[58] P. S. Lum, S. B. Godfrey, E. B. Brokaw, R. J. Holley, and D. Nichols, "Robotic approaches for rehabilitation of hand function after stroke," *American Journal of Physical Medicine & Rehabilitation*, vol. 91, no. 11, pp. S242–S254, 2012.

[59] G. Kwakkel, B. J. Kollen, J. van der Grond, and A. J. Prevo, "Probability of regaining dexterity in the flaccid upper limb impact of severity of paresis and time since onset in acute stroke," *Stroke*, vol. 34, no. 9, pp. 2181–2186, 2003.

[60] D. Prattichizzo, G. Salvietti, F. Chinello, and M. Malvezzi, "An object-based mapping algorithm to control wearable robotic extra-fingers," in *Proc. IEEE/ASME Int. Conf. on Advanced Intelligent Mechatronics*, (Besançon, France), 2014.

[61] D. Prattichizzo, M. Malvezzi, I. Hussain, and G. Salvietti, "The sixth-finger: a modular extra-finger to enhance human hand capabilities," in *Proc. IEEE Int. Symp. in Robot and Human Interactive Communication*, (Edinburgh, United Kingdom), 2014.

[62] I. Hussain, G. Salvietti, L. Meli, C. Pacchierotti, and D. Prattichizzo, "Using the robotic sixth finger and vibrotactile feedback for grasp compensation in chronic stroke patients," in *Proc. IEEE/RAS-EMBS International Conference on Rehabilitation Robotics (ICORR)*, 2015.

[63] G. Salvietti, I. Hussain, D. Cioncoloni, S. Taddei, S. Rossi, and D. Prattichizzo, "Compensating hand function in chronic stroke patients through the robotic sixth finger," *Transaction on Neural System and Rehabilitation Engineering*, 2016.

[64] I. Hussain, G. Spagnoletti, C. Pacchierotti, and D. Prattichizzo, "A wearable haptic ring for the control of extra robotic fingers," in *Proc. Asia Haptics*, (Chiba, Japan), 2016.

[65] A. Hussain, A. Budhota, C. M. L. Hughes, W. D. Dailey, D. A. Vishwanath, C. W. Kuah, L. H. Yam, Y. J. Loh, L. Xiang, K. S. Chua, E. Burdet, and D. Campolo, "Self-paced reaching after stroke: A quantitative assessment of longitudinal and directional sensitivity using the H-man planar robot for upper limb neurorehabilitation," *Front. Neurosci.*, vol. 10, no. OCT, 2016.

[66] Q. Meng and M. H. Lee, "Design issues for assistive robotics for the elderly," *Advanced engineering informatics*, vol. 20, no. 2, pp. 171–186, 2006.

[67] J. L. Pons, "Rehabilitation exoskeletal robotics," *Engineering in Medicine and Biology Magazine, IEEE*, vol. 29, no. 3, pp. 57–63, 2010.

[68] C. A. Stanger, C. Anglin, W. S. Harwin, and D. P. Romilly, "Devices for assisting manipulation: a summary of user task priorities," *Rehabilitation Engineering, IEEE Transactions on*, vol. 2, no. 4, pp. 256–265, 1994.

[69] J. Miguelez, M. Miguelez, and R. Alley, "Amputations about the shoulder: prosthetic management," *Altas of Amputations and Limb DeficienciesSurgical, Prosthetic, and Rehabilitation Principles. Rosemont, IL: American Academy or Orthopaedic Surgeons*, pp. 263–273, 2004.

[70] B. Vanderborght, A. Albu-Schäffer, A. Bicchi, E. Burdet, D. G. Caldwell, R. Carloni, M. Catalano, O. Eiberger, W. Friedl, G. Ganesh, *et al.*, "Variable impedance actuators: A review," *Robotics and autonomous systems*, vol. 61, no. 12, pp. 1601–1614, 2013.

[71] M. Manti, T. Hassan, G. Passetti, N. d'Elia, M. Cianchetti, and C. Laschi, *Biomimetic and Biohybrid Systems: 4th International Conference, Living Machines 2015, Barcelona, Spain, July 28 - 31, 2015, Proceedings*, ch. An Under-Actuated and Adaptable Soft Robotic Gripper, pp. 64–74. Cham: Springer International Publishing, 2015.

[72] A. M. Dollar and R. D. Howe, "Joint coupling design of underactuated hands for unstructured environments," *The International Journal of Robotics Research*, vol. 30, no. 9, pp. 1157–1169, 2011.

[73] C. Laschi and M. Cianchetti, "Soft robotics: new perspectives for robot bodyware and control," *Frontiers in bioengineering and biotechnology*, vol. 2, no. 3, 2014.

[74] L. Birglen, T. Lalibertè, and C. Gosselin, *Underactuated Robotic Hands*, vol. 40 of *Springer Tracts in Advanced Robotics*. Springer, 2008.

[75] A. M. Dollar and R. D. Howe, "The highly adaptive sdm hand: Design and performance evaluation," *The international journal of robotics research*, vol. 29, no. 5, pp. 585–597, 2010.

[76] C. Eppner and O. Brock, "Grasping unknown objects by exploiting shape adaptability and environmental constraints," in *Intelligent Robots and Systems (IROS), 2013 IEEE/RSJ International Conference on*, pp. 4000–4006, Nov 2013.

[77] M. G. Catalano, G. Grioli, E. Farnioli, A. Serio, C. Piazza, and A. Bicchi, "Adaptive synergies for the design and control of the pisa/iit softhand," *The International Journal of Robotics Research*, vol. 33, no. 5, pp. 768–782, 2014.

[78] ArbotiX, "Arbotix-m robocontroller,open source," 2012. On-line: http://www.trossenrobotics.com/p/arbotix-robot-controller.aspx.

[79] F. Wu and H. Asada, "Bio-artificial synergies for grasp posture control of supernumerary robotic fingers," in *Proceedings of Robotics: Science and Systems*, (Berkeley, USA), July 2014.

[80] G. Gioioso, G. Salvietti, M. Malvezzi, and D. Prattichizzo, "Mapping synergies from human to robotic hands with dissimilar kinematics: an approach in the object domain," *IEEE Trans. on Robotics*, 2013.

[81] L. Meli, C. Pacchierotti, and D. Prattichizzo, "Sensory subtraction in robot-assisted surgery: fingertip skin deformation feedback to ensure safety and improve transparency in bimanual haptic interaction," *IEEE Transactions on Biomedical Engineering*, vol. 61, no. 4, pp. 1318–1327, 2014.

[82] C. Pacchierotti, D. Prattichizzo, and K. J. Kuchenbecker, "Cutaneous feedback of fingertip deformation and vibration for palpation in robotic surgery," *IEEE Transactions on Biomedical Engineering*, vol. 63, no. 2, pp. 278–287, 2016.

[83] C. Pacchierotti, *Cutaneous haptic feedback in robotic teleoperation*. Springer Series on Touch and Haptic Systems, Springer International Publishing, 2015.

[84] S. M. Son, Y. H. Kwon, N. K. Lee, S. H. Nam, and K. Kim, "Deficits of movement accuracy and proprioceptive sense in the ipsi-lesional upper limb of patients with hemiparetic stroke," *Journal of physical therapy science*, vol. 25, no. 5, p. 567, 2013.

[85] N. M. F. V. Lima, K. C. Menegatti, É. Yu, N. Y. Sacomoto, T. B. Scalha, I. N. D. F. Lima, S. M. A. d. Camara, M. C. d. Souza, R. d. O. Cacho, E. W. d. A. Cacho, *et al.*, "Sensory deficits in ipsilesional upper-extremity in chronic stroke patients," *Arquivos de neuro-psiquiatria*, pp. 1–6, 2015.

[86] C. Pacchierotti, G. Salvietti, I. Hussain, L. Meli, and D. Prattichizzo, "The hRing: a wearable haptic device to avoid occlusions in hand tracking," in *Proc. IEEE Haptics Symposium (HAPTICS)*, 2016.

[87] M. Zecca, S. Micera, M. Carrozza, and P. Dario, "Control of multifunctional prosthetic hands by processing the electromyographic signal," *Critical Reviews in Biomedical Engineering*, vol. 30, no. 4-6, 2002.

[88] K. Kiguchi, T. Tanaka, and T. Fukuda, "Neuro-fuzzy control of a robotic exoskeleton with emg signals," *Fuzzy Systems, IEEE Transactions on*, vol. 12, no. 4, pp. 481–490, 2004.

[89] A. Brodal, *Neurological anatomy in relation to clinical medicine*. Oxford University Press, USA, 1981.

[90] D. Farina and R. Merletti, "Comparison of algorithms for estimation of emg variables during voluntary isometric contractions," *Journal of Electromyography and Kinesiology*, vol. 10, no. 5, pp. 337–349, 2000.

[91] B. Çalli, A. Walsman, A. Singh, S. Srinivasa, P. Abbeel, and A. M. Dollar, "Benchmarking in manipulation research: The YCB object and model set and benchmarking protocols," *CoRR*, vol. abs/1502.03143, 2015.

[92] J. Falco, K. Van Wyk, S. Liu, and S. Carpin, "Grasping the performance: Facilitating replicable performance measures via benchmarking and standardized methodologies," *Robotics & Automation Magazine, IEEE*, vol. 22, no. 4, pp. 125–136, 2015.

[93] M. Ciocarlie and P. Allen, "A design and analysis tool for underactuated compliant hands," in *Intelligent Robots and Systems, 2009. IROS 2009. IEEE/RSJ International Conference on*, pp. 5234 –5239, oct. 2009.

[94] S. Krut, V. Bégoc, E. Dombre, and F. Pierrot, "Extension of the form closure property to underactuated hands," *IEEE Transactions on Robotics*, vol. 26, pp. 853–866, 2010.

[95] T. Brott, H. Adams, C. P. Olinger, J. R. Marler, W. G. Barsan, J. Biller, J. Spilker, R. Holleran, R. Eberle, and V. Hertzberg, "Measurements of acute cerebral infarction: a clinical examination scale.," *Stroke*, vol. 20, no. 7, pp. 864–870, 1989.

[96] A. Heller, D. Wade, V. A. Wood, A. Sunderland, R. L. Hewer, and E. Ward, "Arm function after stroke: measurement and recovery over the first three months.," *Journal of Neurology, Neurosurgery & Psychiatry*, vol. 50, no. 6, pp. 714–719, 1987.

[97] R. Bogue, "Exoskeletons and robotic prosthetics: a review of recent developments," *Industrial Robot: An International Journal*, vol. 36, no. 5, pp. 421–427, 2009.

[98] D. H. Stefanov, Z. Bien, and W.-C. Bang, "The smart house for older persons and persons with physical disabilities: structure, technology arrangements, and perspectives," *IEEE transactions on neural systems and rehabilitation engineering*, vol. 12, no. 2, pp. 228–250, 2004.

[99] L. Hoyet, F. Argelaguet, C. Nicole, and A. Lécuyer, "wow! i have six fingers!: Would you accept structural changes of your hand in vr?," *Frontiers*, vol. 3, no. 27, p. 1, 2016.